Global Survey of miRNAs and tRNA-derived Small RNAs From Human Parasitic Protist Trichomonas Vaginalis

Zhensheng Wang
Chinese Academy of Medical Sciences and Peking Union Medical College https://orcid.org/0000-0003-2708-0656

Hongchang Zhou
Huzhou University

Chunyan Wei
Chinese Academy of Medical Sciences & Peking Union Medical College Institute of Biomedical Engineering

Zhihua Wang
Department of immunology, Guilin medical university

Xiao Hao
blood station of Jinan

Lianhui Zhang
Chinese academy of medical sciences

Jingzhong Li
NHC key laboratory of echinococcosis prevention and control

Zenglei Wang (zengleiwang@pumc.edu.cn)
NHC Key Laboratory of Systems Biology of Pathogens, Institute of Pathogen Biology, Chinese Academy of Medical Sciences and Peking Union Medical College, Beijing, People's Republic of China

Heng Wang
Chinese academy of medical sciences

Research

Keywords: Trichomonas vaginalis, transfer RNA, tRNA-derived small RNAs, tRFs, tRNA-halves, trichomoniasis

Posted Date: November 5th, 2020

DOI: https://doi.org/10.21203/rs.3.rs-101825/v1

Version of Record: A version of this preprint was published on January 29th, 2021. See the published version at https://doi.org/10.1186/s13071-020-04570-9.

Abstract

Background

Small non-coding RNAs play critical regulatory roles in post-transcription. However, their characteristics in *Trichomonas vaginalis* (*T. vaginalis*), the causative agent of human sexually transmitted trichomoniasis, still remain to be unveiled.

Methods

Small RNA transcriptomes from *Trichomonas* trophozoites were deeply sequenced through Illumina NextSeq 500 system and comprehensively analyzed to identify *Trichomonas* miRNAs and tRNA-derived small RNAs (tsRNAs). The tsRNAs candidates were confirmed by stem-loop RT-PCR and motifs to guide the cleavage of tsRNAs were predicted by performing GLAM2 algorithm.

Results

The miRNAs were found at extremely low abundance (0.0046%) in *T. vaginalis*. Three categories of endogenous *Trichomonas* tsRNAs were identified as 5'tritsRNAs, mid-tritsRNAs and 3'tritsRNAs, with 5'tritsRNAs dominating (67.63%) in tsRNAs. Interestingly, the cleavage site analysis verified both conventional classes of tRFs and tRNA-halves in tritsRNAs, indicating the expression of tRNA-halves in non-stress condition. A total of 25 tritsRNAs were experimentally confirmed, accounting for 78.1% of all tested candidates. Three motifs were predicted to guide the production of tritsRNAs. This proved the expression of tRFs and tRNA-halves in *T. vaginalis* transcriptome.

Conclusions

This is the first report of genome-wide investigation of small RNAs, particularly tsRNAs and miRNAs, from *Trichomonas* parasites. Our findings demonstrate the expression profile of tsRNAs in *T. vaginalis*, while miRNA was hardly discovered. These results might promote the further research to better understand the evolution of small non-coding RNA in *T. vaginalis* and their functions in pathogenesis of trichomoniasis.

Background

Small noncoding RNAs (snRNAs) have emerged as essential post-transcriptional regulators in a myriad of cellular and organismal processes, and thus become an important research focus in the past three decades. Since the discovery of microRNAs (miRNAs) in 1993 [1], the repertoire of snRNAs has greatly expanded through continuous characterization of new small RNAs from various origins facilitated by the advance of deep sequencing technologies. Aside from the well-established snRNAs such as miRNAs, endogenous small interference RNAs (endosiRNAs) and P-element induced wimpy testis (PIWI) protein-interacting RNAs (piRNAs), transfer RNA (tRNA)-derived snRNAs remain a highly studied topic in recent years, and their important roles in a wide variety of biological and pathological situations have been increasingly recognized.

tRNA-derived small RNAs (tsRNAs) can be broadly categorized into two main classes likely depending on their biogenesis: tRNA-halves and tRNA-derived fragments (tRFs). The conventional tRNA-halves are produced by a single ribonucleolytic cleavage within the anticodon loops of mature tRNAs under stress conditions, and thus they have also been referred to as tRNA-derived stress-induced small RNAs (tiRNAs) [2, 3, 4, 5, 6]. However, a recent study presented evidence of tRNA-halves expression in non-stress condition [7], yet factors affecting the genesis of tRNA-halves might need to be re-evaluated. Endonucleolytic cleavages of both mature and precursor tRNAs near the D-□anticodon-□or TψC-arm lead to the generation of tRFs. Despite the nomenclature to describe the types of tRFs is to be consistent, they are typically classified into four subclasses: 5'tRFs, 3'tRFs (or 3'CCA tRFs), 3'UtRFs (tRF-1), and internal tRFs (itRFs or mid-tRFs) in terms of their positions mapped to tRNAs [8, 9, 10]. tRFs are constitutively and conservatively expressed in organisms from lower archaea to mammals, however, their biological roles and mechanisms of action remain largely unclear.

Research to date has associated tsRNAs with diverse human diseases and infections, revealing their functions in regulation of cell apoptosis, cell viability, RNA degradation, RNA stability, translational repression and cellular proliferation [6, 11, 12, 13, 14]. Most interestingly, tRFs hold the ability to behave like canonical miRNAs and regulate target gene expression through essential interactions with Argonaute (AGO) families [15, 16], PIWI [17], or DICER proteins [18]. The similarity of tRFs and miRNAs also resulted in misannotation and cross-mapping of these two groups. In some species lack of miRNA molecules, such as *Plasmodium* parasites, tRFs might act as alternative regulators to accomplish the intense post-transcriptional regulation needed during the rapid morphological change [10]. In flagellated protozoan *Giardia lamblia*, the abundant tRFs were involved in the differentiation process, while the previously reported miRNAs were found absent or misannotated [19]. tRFs have also been discovered from other protozoan parasites, including *Tetrahymena* , *Trypanosoma cruzi* [20], as well as from exosomes of *leishmania donovani* [21], implying their conservative expression in primitive eukaryotes, although their functions need to be further investigated.

Trichomonas vaginalis is an extracellular, unicellular flagellated protozoan parasite that belongs to the same class of Zoomastigophorea as *G. lamblia*. Infection of *T. vaginalis* leads to the occurrence of trichomoniasis, which remains as the most prevalent non-viral sexually transmitted disease and afflicts 142.6 million people annually [22]. *T. vaginalis* parasites undergo dramatic biological changes even within the single trophozoite stage, including morphological change, DNA replication, multiple nucleus divisions, transposon activities and lateral gene transfer during differentiation. It is possible that the parasites take the advantage of certain snRNAs, such as tRNA-halves, tRFs or miRNAs, in the complicated manipulations. As yet, miRNAs were only reported by *in silico* prediction or hairpin-loop searching from *T. vaginalis* [23, 24, 25], however, the misinterpretation of miRNAs discovered by the same methods in a closely related parasite, *G. lamblia* [19], hinted at an ambiguous fate of *Trichomonas* miRNA molecules. Albeit a recent study revealed the occurrence of nine tRNA-halves in extracellular vesicles from *T. vaginalis* [7], their global expression profile in this parasite still remains to be revealed. It is therefore necessary to revisit the small RNAs in *T.vaginalis*, in particular tsRNAs and miRNAs, by the advanced high-throughput deep sequencing to achieve more understandings to snRNAs in this parasite.

We deeply sequenced small RNA transcriptome from *Trichomonas* trophozoites. By genome-wide comprehensive analysis and experimental verification, we report for the first time the global identification and characterization of endogenous *Trichomonas* tsRNAs, which may hold a pivotal role in parasite development. However, miRNA was hardly discovered in our sequencing data.

Methods

T. vaginalis maintenance and RNA isolation

Three clones (Tv01, Tv02 and Tv03) of *T. vaginalis* laboratory strain P7 were maintained in Diamond's media supplemented with 10% heat-inactivated bovine serum, penicillin (100 units/ml) and streptomycin (0.1mg/ml) at 37°C as previously described [26]. The parasite viability and density were monitored by Trypan blue exclusion on hemocytometer. Less than 1×10^6 trophozoites/ml was maintained during culture to avoid overgrowth. The pellet of each isolate was collected at exponential phase of trophozoite by centrifugation. Total RNA was extracted employing TRIzol Reagent (Invitrogen, Shanghai, China) and treated with DNase I to remove any genomic DNA contamination. RNA was then separated by urea-denatured 15% polyacrylamide gel electrophoresis, and bands of small RNAs with the length of 12–40 nucleotides (nt) were extracted and purified for further use.

Small RNA library construction and deep sequencing

To avoid the interference of numerous post-transcriptional modifications in tRNA along complementary DNA (cDNA) synthesis and adapter ligation in RNA-seq, the following treatments were completed before library construction: both 3'-aminoacyl deacylation and 2', 3'-cyclic phosphate removal to 3'-OH for 3' adaptor ligation, 5'-hydroxyl group phosphorylation to 5'-phosphorylation for 5'-adaptor ligation, and m1A and m3C demethylation for efficient reverse transcription. Small RNA libraries construction and sequencing were accomplished following the commercial protocols. Briefly, small RNA molecules were ligated to 5' and 3' adaptors consecutively and then converted to cDNA by reverse transcription followed by polymerase chain reaction (PCR) amplifications. Approximately 2.34 femtomole of reverse transcription - PCR (RT-PCR) products per sample were sequenced directly by Illumina NextSeq 500 system (Illumina, USA) at 50 base pairs (bp) single-read by Aksomics Inc (Shanghai, China).

Small RNA analysis and tsRNAs identification

The quality of raw sequencing data was evaluated by FastQC (v0.11.7). The 3' and 5' adaptors were trimmed and reads shorter than 18 nt or longer than 40 nt were filtered out by Cutadapt (v1.17) and Python2 (v2.7.5) to remove any contamination and yielded the clean data. The clean dataset was further mapped to the genome of *T. vaginalis* G3 strain (TrichDB, release 47, http://trichdb.org/trichdb/) using BLASTN. The clean-read counts were normalized as a relative number per one million reads (RPM) and analyzed in both total and unique read categories to indicate the abundance and diversity of reads, respectively. To investigate tRNA derived segments, the data were further aligned to a total of 165 *T. vaginalis* tRNA genes downloaded from TrichDB database (http://trichdb.org/trichdb/) by performing

BLASTN alignment. The genome-wide expression intensity of the *T. vaginalis* tsRNAs was sequentially calculated with the “Build” function of Bowtie2 (v2.1.0.0) and the “coverageBed” function of Bedtools (v2.29.2). Data extraction of each type of tsRNAs was performed by compiled Perl (v5.22) codes. The statistical analysis for the Pearson correlation coefficients was carried out utilizing the “cor” function in R package stats. The ggplot2 package (v3.3.1) in R language (v3.5.0) was employed to create all the plots.

Motif analysis

The motifs at the cleavage sites of tritsRNAs were predicted by exploiting the GLAM2 algorithm in Gapped Local Alignment of Motifs (GLAM2 v1056) [22] with default parameters adopted, except that only the given strand was aligned.

Stem-loop RT-PCR

The templates of total RNAs were reverse-transcribed into cDNAs utilizing the Goldenstar^{TM} RT6 cDNA Synthesis Kit (Beijing TsingKe Biotech Co. Ltd., Beijing, China) following the manufacturer’s instruction. Specific stem-loop reverse transcription primers (Additional file 1: Table S1) were designed in accordance with the sequence of each tritsRNA candidates, as described previously [27, 28]. The PCR was carried out with an initial denaturation at 98°C for 2 min, followed by 35 cycles of denaturation at 98°C for 10 s, annealing at 55°C for 10 s and extension at 72°C for 15 s, and a final extension at 72°C for 5 min. The PCR products were evaluated on 12% polyacrylamide gel. The expected sizes of the PCR products were estimated by the length of each tsRNAs with additional ~40 bp of nucleotides technically introduced in the stem-loop primers. Negative controls lacking of DNase I - treated RNA or reverse transcriptase in RT reactions, or template in PCR were applied to validate the accuracy and specificity of stem-loop RT-PCR. The PCR primers were listed in Additional file 1: Table S2.

Results

Absence of miRNAs in *T. vaginalis*

Three *T. vaginalis* strains were employed for deeply sequencing the 18-40 nt small RNAs. As showed in Table 1, the three libraries yielded 6 303 530, 7 071 840, and 5 809 794 reads that perfectly mapped to the *T. vaginalis* genome, respectively, accounting for an average of 91.76% of the clean data. The distribution of mapped reads from these three isolates was relatively consistent, all displaying three main peaks at the size 29, 32 and 36 nt (Fig. 1a). Therefore, these data were pooled together for further analysis to enhance the identification of novel type of small RNAs. Apart from the three key peaks as expected in total reads, a single peak at 34 nt showed in unique reads (Fig. 1b). Such feature was incredibly different from those of model organisms, which generally demonstrated a peak at ~22 nt dominated by miRNAs in both total and unique read aspects [29, 30, 31]. This suggested that the composition of small RNAs in *T. vaginalis* might be divergent.

The data were then annotated and the abundance of each type of small RNAs was assessed for its expression level. As illustrated in Fig. 1c, these small RNAs were originated from ribosomal RNAs (rRNAs), tRNAs, messenger RNAs (mRNAs), small nuclear RNAs (snRNAs) / small nucleolar RNAs (snoRNAs), as well as unannotated small RNAs. Unexpectedly, miRNAs in our pool showed at extremely low abundance (0.0046%). Among the 27 miRNAs identified previously [23, 24, 25], only nine were detected in our deep sequencing data with particular low counts, except for one namely 'tvm-005' derived from tRNA (Additional file 1: Table S3). In contrast, tsRNAs predominated after rRNA-derived reads and accounted for 12.79% of clean reads. These molecules prevailed in *T. vaginalis* genomic contig DS113177 to DS127907, from where tRNA genes were mainly coded (Fig. 1d).

Profiles of tsRNAs from *T. vaginalis*

To explore the expression profiles of tsRNAs, their parental tRNAs consisting of 20 amino acids were analyzed. Eight amino acids, including Glu, Gly, Phe, Lys, Val, Arg, Asn, and Tyr, were found to produce up to 85% of tsRNAs (Fig. 2a). Such expression bias indicated that tsRNAs were not generated by random degradation of mature tRNAs. The distribution pattern of tsRNAs was further investigated. Other than that in Fig. 1b, it showed only two conspicuous peaks dominating at ~29 and ~33 nt in total tsRNAs (Fig. 2b), implying multiple types of tsRNAs with diverse sizes in *T. vaginalis*. These tsRNA reads were therefore mapped to all 165 *Trichomonas* tRNAs. As expected, their biogenesis from the parental tRNAs were found relatively conserved as previously reported [10, 19, 20, 21], with a large amount of reads aligned to three main positions at 5' end, anticodon area and 3' end of mature tRNAs (Fig. 2c). Consequently, these three types of *Trichomonas* tsRNAs were named as 5'tritsRNAs, mid-tritsRNAs and 3'tritsRNAs, respectively. The homogeneity of these tritsRNAs based on their types and size distributions were investigated by plotting the RPM values against sizes in both total and unique reads. Two peaks were observed for 5'tritsRNAs at ~29 nt and ~33 nt, for mid-tritsRNAs at ~21/22 nt, and for 3'tritsRNAs at ~24 nt and ~40 nt, respectively (Fig. 2d), displaying great difference in their sizes. The double peaks occurred in the plots of 5'tritsRNAs and 3'tritsRNAs suggested that there were at least two subgroups of tritsRNAs in each.

We subsequently selected the top 20 tRNAs that produced high level of tritsRNAs to further evaluate their expression divergence. Among them, seven primarily produced 5'tritsRNAs, three generated mid-tritsRNAs and five created 3'tritsRNAs, and the rest yielded tritsRNAs from multiple regions (Fig. 2c). 5'tritsRNAs prevailed (67.62%) in tritsRNAs, whereas mid-tritsRNAs and 3'tritsRNAs accounted for only 7.37% and 15.86%, respectively (Fig. 2e). No significant association between the abundance of any two types of tritsRNAs was found by Pearson correlation analysis (Additional file 2: Figure S1). The predominated tritsRNAs in each group were then examined by plotting the RPM values of all 60 tritsRNAs from these tRNAs against their sizes. A total of 32 tritsRNAs were identified to show consistent peaks as in Fig. 2d, including nine 5'tritRFs, twelve mid-tritsRNAs, and eleven 3'tritRFs, as displayed in Additional file 3, 4 and 5: Figure S2, S3, S4 and Table 2. Consequently, these 32 tritsRNAs were employed for further classification and confirmation analysis.

Identification of tritRFs and tritRNA-halves

Given that tRFs, typically shorter than 32 nt [8], are the theoretical products of tRNA-derived small RNAs under ordinary condition, our analysis identified longer products in both 3' and 5'tritsRNAs. To further classify these tritsRNAs, we investigated their cleavage sites by aligning each of those 32 tritsRNAs to its parental tRNA. As illustrated in Fig. 3, two sites were identified to produce 5'tritsRNAs, with one occurring in the anticodon loop to generate those of 33 nt, and one in the anticodon arm to yield these of 29 nt. The mid-tritsRNAs originated from two sets of combined endonucleolytic cleavages both in the arms neighboring to anticodon loop and TψC loop, however, one group covered the anticodon loop while the other involved the TψC loop. Three cleavage sites in anticodon loop, anticodon arm and TψC arm resulted in the generation of 3'tritsRNAs with sizes of 40, 33 and 24 nt, respectively. Therefore, 5'tritsRNAs of 29 nt, mid-tritsRNAs and 3'tritsRNAs of 24/33 nt were produced by combined cleavages other than in the anticodon loop and belonged to the class of tritRFs. While two types (5'tritsRNAs of 33 nt and 3'tritRNAs of 40 nt) were generated by single cleavage in the anticodon loop and thus were classified as tritRNA-halves (Table 2).

Experimental confirmation of tritsRNA candidates and motif prediction

We further experimentally evaluated the presence of tritRFs and tritRNA-halves in *T. vaginalis* to confirm our findings. Stem-loop RT-PCR successfully amplified 25 (nine 5'tritsRNAs, seven mid-tritsRNAs, and nine 3'tritsRNAs) of these 32 candidates, corresponding to 78.1% of tested candidates. This proved the expression of both tritRFs and tritRNA-halves in *T. vaginalis* transcriptome (Fig. 4a).

The motifs around the cleavage sites that might guide the generation of tritsRNAs were then explored. By employing GLAM2 algorithm, three motifs (Motif TV1-3, Fig. 4b) were successfully predicted to process tritsRNAs. Motif TV1 was located along D-stem and anticodon-arm for the 3' end cleavage of 5'tritsRNAs (29 nt). Motif TV2 and TV3 were both in TψC stem to process the 3' end cleavage of mid-tritsRNAs (22 nt) and 5' end cleavage of 3'tritsRNAs (24 nt), respectively. Albeit both motif TV2 and TV3 contained highly conservative ‘UUC’ triple-nucleotide element, they seemed to take charge of generating various types of tritsRNAs (Fig. 4b).

Discussion

Despite the critical regulatory roles of small non-coding RNAs in post-transcription, our knowledge on their characteristics, biogenesis and functions in lower eukaryotes remains to be increased. The recent rapid development of high-throughput sequencing technology has greatly advanced researches on small non-coding RNAs, yet a variety of small RNAs have been unveiled, including those formerly misclassified tRNA-derived small RNAs. In this study, we took the advantage of deep sequencing techniques and genome-widely investigated small RNAs from human infected parasite *T. vaginalis*. Strikingly, miRNA occurred at particularly low abundance (0.0046%) in our dataset. Although previous studies have reported 27 miRNAs using *in silico* prediction or hairpin-loop searching, only nine were identified in our analysis. Two of them were derived from tRNAs and classified as 5'tritsRNA-Gln^{TTG} and 5'tritsRNA-Thr^{TGT}, and one was apparently generated from 16s ribosomal RNA [23]. Given that miRNA occurred at extremely low

abundance, they might play little biological role or even not present in *T. vaginalis*. It seems common that miRNA is absent or has no biological function in protist such as *Plasmodium falciparum* [10], *Giardia lamblia* [19] and *Leishmania* parasites [32]. Thereby, these parasites likely employ other molecules to complete gene regulation. For instance, tsRNAs have been reported to be involved in *Giardia lamblia* parasite differentiation [19].

In *T. vaginalis*, we identified three categories of tritsRNAs: 5'tritsRNAs, mid-tritsRNAs and 3'tritsRNAs. Of interest, both tRFs and tRNA-halves were classified from these tritsRNAs. This is the first time to report both tRFs and tRNA-halves from a protist organism under ordinary culture condition. tRNA-halves are generally believed to be the products of tRNAs under nutritional, biological or physicochemical stresses, however, our experiment involved no stress during *T. vaginalis* parasite culture. Such phenomenon has also been noticed in a recent study, where nine tRNA-halves were discovered from extracellular vesicles of *T. vaginalis* parasite under no external stress [7]. These distinctive features suggested that tsRNAs might play a unique role in the developmental process of *T. vaginalis.*

The mechanisms of tsRNAs biogenesis have yet to be revealed because the cleavage loci of those known tRNA-specific nucleases still remain to be fully addressed. We therefore analyzed the motifs for tritsRNAs production. Since tRNA structure is highly conserved, there might be other factors involved in the genesis of tritsRNAs. In a tRNA, D- and T-loop interact with each other to support the stabilization. It is thus possible that the motifs might be dependent on spatial structure of tRNA and composed with nucleotides that were not adjacent to each other along the sequence. Other unknown mechanisms might also take place in addition to motif recognition in tritsRNAs generation and need to be further elucidated.

Conclusions

Taken together, this study has provided the first comprehensive evaluation of small non-coding RNAs in *T. vaginalis*. The previously reported miRNAs were not discovered, indicating the absence or little biological function of miRNAs in *T. vaginalis* parasites. Interestingly, three categories of tritsRNAs composed of both classes of tritRFs and tritRNA-halves were identified from *T. vaginalis* under no stress condition. Future research is needed to understand whether these tsRNAs play a particular role in *T. vaginalis*. Our findings demonstrate the profile of small RNAs and provide the evidence of tRFs and tRNA-halves in *T. vaginalis*, which could lead to better understanding of the evolution of RNA processing in the early eukaryotes and the pathogenesis of trichomoniasis.

Abbreviations

tsRNAs: Transfer RNA derived small RNAs; snoRNA: Small nucleolar RNA; snRNA: Small nuclear RNA; tRFs: Transfer RNA derived fragments; AGO: Argonaute protein; cDNA: Complementary DNA; DNA: Deoxyribonucleic acid; miRNA: MicroRNA; ncRNA: Non-coding RNA; PiWi-interacting RNA; PiWi: P-element induced wimpy testis; RNA: Ribonucleic acid; RPM: Relative number per one million reads; rRNA: Ribosomal RNA; RT-PCR: Quantitative reverse-transcribed polymerase chain reaction

Declarations

Funding

This work has been supported by CAMS Innovation Fund for Medical Sciences (CIFMS) (2017-I2M-3-016), NHC Key Laboratory of Echinococcosis Prevention and Control (2020WZK2009), and The Key Laboratory of Vector Biology and Pathogen Control of Zhejiang Province, Huzhou University (Grant No. HUZUL201908).

Authors' contributions

WZS, ZHC, WCY, ZLH, WZH, HX conceived and designed the experiments. WZS, WZL performed the experiments. WZS, WZL, LJZ analyzed the data. WZS, WZL, WH wrote the manuscript. All authors read and approved the final manuscript.

Availability of data and materials

The datasets generated and analyzed during the current study are available in the GEO repository under the accession number GSE160464.

Ethics approval and consent to participate

This work was not involved in ethics approval.

Consent for publication

Not applicable.

Competing interests

The authors declare that they have no competing interests.

References

1. Lee RC, Feinbaum RL, Ambros V. The C. elegans heterochronic gene lin-4 encodes small RNAs with antisense complementarity to lin-14. Cell. 1993;75:843-54.
2. Fu H, Feng J, Liu Q, Sun F, Tie Y, Zhu J, et al. Stress induces tRNA cleavage by angiogenin in mammalian cells. FEBS Lett. 2009;583:437-42.
3. Thompson DM, Parker R. The RNase Rny1p cleaves tRNAs and promotes cell death during oxidative stress in Saccharomyces cerevisiae. J Cell Biol. 2009;185:43-50.
4. Thompson DM, Parker R. Stressing out over tRNA cleavage. Cell. 2009;138:215-9.
5. Chen Q, Yan M, Cao Z, Li X, Zhang Y, Shi J, et al. Sperm tsRNAs contribute to intergenerational inheritance of an acquired metabolic disorder. Science. 2016;351:397-400.

6. Saikia M, Jobava R, Parisien M, Putnam A, Krokowski D, Gao XH, et al. Angiogenin-cleaved tRNA halves interact with cytochrome c, protecting cells from apoptosis during osmotic stress. Mol Cell Biol. 2014;34:2450-63.
7. Artuyants A, Campos TL, Rai AK, Johnson PJ, Dauros-Singorenko P, Phillips A, et al. Extracellular vesicles produced by the protozoan parasite Trichomonas vaginalis contain a preferential cargo of tRNA-derived small RNAs. Int J Parasitol. 2020.
8. Keam SP, Hutvagner G. tRNA-Derived Fragments (tRFs): Emerging New Roles for an Ancient RNA in the Regulation of Gene Expression. Life (Basel). 2015;5:1638-51.
9. Kumar P, Kuscu C, Dutta A. Biogenesis and Function of Transfer RNA-Related Fragments (tRFs). Trends Biochem Sci. 2016;41:679-89.
10. Wang Z, Wei C, Hao X, Deng W, Zhang L, Wang Z, et al. Genome-wide identification and characterization of transfer RNA-derived small RNAs in Plasmodium falciparum. Parasit Vectors. 2019;12:36.
11. Lee YS, Shibata Y, Malhotra A, Dutta A. A novel class of small RNAs: tRNA-derived RNA fragments (tRFs). Genes Dev. 2009;23:2639-49.
12. Cai P, Piao X, Hao L, Liu S, Hou N, Wang H, et al. A deep analysis of the small non-coding RNA population in Schistosoma japonicum eggs. PLoS One. 2013;8:e64003.
13. Sobala A, Hutvagner G. Small RNAs derived from the 5' end of tRNA can inhibit protein translation in human cells. RNA Biol. 2013;10:553-63.
14. Li Z, Ender C, Meister G, Moore PS, Chang Y, John B. Extensive terminal and asymmetric processing of small RNAs from rRNAs, snoRNAs, snRNAs, and tRNAs. Nucleic Acids Res. 2012;40:6787-99.
15. Kumar P, Anaya J, Mudunuri SB, Dutta A. Meta-analysis of tRNA derived RNA fragments reveals that they are evolutionarily conserved and associate with AGO proteins to recognize specific RNA targets. BMC Biol. 2014;12:78.
16. Loss-Morais G, Waterhouse PM, Margis R. Description of plant tRNA-derived RNA fragments (tRFs) associated with argonaute and identification of their putative targets. Biol Direct. 2013;8:6.
17. Keam SP, Young PE, McCorkindale AL, Dang TH, Clancy JL, Humphreys DT, et al. The human Piwi protein Hiwi2 associates with tRNA-derived piRNAs in somatic cells. Nucleic Acids Res. 2014;42:8984-95.
18. Cole C, Sobala A, Lu C, Thatcher SR, Bowman A, Brown JW, et al. Filtering of deep sequencing data reveals the existence of abundant Dicer-dependent small RNAs derived from tRNAs. RNA. 2009;15:2147-60.
19. Liao JY, Guo YH, Zheng LL, Li Y, Xu WL, Zhang YC, et al. Both endo-siRNAs and tRNA-derived small RNAs are involved in the differentiation of primitive eukaryote Giardia lamblia. Proc Natl Acad Sci U S A. 2014;111:14159-64.
20. Reifur L, Garcia-Silva MR, Poubel SB, Alves LR, Arauco P, Buiar DK, et al. Distinct subcellular localization of tRNA-derived fragments in the infective metacyclic forms of Trypanosoma cruzi. Mem Inst Oswaldo Cruz. 2012;107:816-9.

21. Lambertz U, Oviedo Ovando ME, Vasconcelos EJ, Unrau PJ, Myler PJ, Reiner NE. Small RNAs derived from tRNAs and rRNAs are highly enriched in exosomes from both old and new world Leishmania providing evidence for conserved exosomal RNA Packaging. BMC Genomics. 2015;16:151.
22. WHO: Report on global sexually transmitted infection surveillance 2015. World Health Organization; 2016.
23. Huang PJ, Lin WC, Chen SC, Lin YH, Sun CH, Lyu PC, et al. Identification of putative miRNAs from the deep-branching unicellular flagellates. Genomics. 2012;99:101-7.
24. Chen XS, Collins LJ, Biggs PJ, Penny D. High throughput genome-wide survey of small RNAs from the parasitic protists Giardia intestinalis and Trichomonas vaginalis. Genome Biol Evol. 2009;1:165-75.
25. Lin WC, Li SC, Lin WC, Shin JW, Hu SN, Yu XM, et al. Identification of microRNA in the protist Trichomonas vaginalis. Genomics. 2009;93:487-93.
26. Diamond LS. The establishment of various trichomonads of animals and man in axenic cultures. J Parasitol. 1957;43:488-90.
27. Chen C, Ridzon DA, Broomer AJ, Zhou Z, Lee DH, Nguyen JT, et al. Real-time quantification of microRNAs by stem-loop RT-PCR. Nucleic Acids Res. 2005;33:e179.
28. Kramer MF. Stem-loop RT-qPCR for miRNAs. Curr Protoc Mol Biol. 2011;Chapter 15:Unit 15 0.
29. Ji X, Jiang P, Luo J, Li M, Bai Y, Zhang J, et al. Identification and characterization of miRNAs involved in cold acclimation of zebrafish ZF4 cells. PLoS One. 2020;15:e0226905.
30. Urena-Peralta JR, Alfonso-Loeches S, Cuesta-Diaz CM, Garcia-Garcia F, Guerri C. Deep sequencing and miRNA profiles in alcohol-induced neuroinflammation and the TLR4 response in mice cerebral cortex. Sci Rep. 2018;8:15913.
31. Warf MB, Johnson WE, Bass BL. Improved annotation of C. elegans microRNAs by deep sequencing reveals structures associated with processing by Drosha and Dicer. RNA. 2011;17:563-77.
32. Atayde VD, Tschudi C, Ullu E. The emerging world of small silencing RNAs in protozoan parasites. Trends Parasitol. 2011;27:321-7.

Tables

Table 1. Mapping and classification of reads against *T. vaginalis* genome

	Tv01	Tv02	Tv03	Pooled data
Clean reads	6909748	7811640	6186244	20907632
Un-mappedReads	606218	739800	375450	1721468
MappedReads	6303530	7071840	5809794	19185164
mRNAs	190790	322082	651191	1164063
5'UTR	3765	5245	7938	16948
CDS	186694	316213	642807	1145714
3'UTR	1219	1648	2095	4962
rRNAs	2772196	2639586	1807762	7219544
tRNAs	955479	1076990	624938	2657407
miRNAs	39596	57388	44879	141863
sn/snoRNAs	1331	1521	1532	4384
UnannotedsmallRNAs	2344138	2974273	2679492	7997903

Table 2. Classification of tritsRNAs candidates

Category	Class	Parental tRNAs	Size(nt)
5'tritsRNAs	5'tritRFs	Glu^{CTC}, Glu^{TTC}, Lys^{CTT}, Lys^{TTT}, Val^{GAC}, Tyr^{GTA}	29
	5'tritRNA-halves	Phe^{GAA}, Gly^{GCC}, Val^{TAC}	33
mid-tritsRNAs	mid-tritRFs	Arg^{CCT}, Arg^{TCT}, Asn^{GTT}, Asp^{GTC}, Gln^{CTG}, His^{GTG}, Ile^{GAT}, Lys^{CTT}, Met^{CAT}, Val^{GAC}, Phe^{AAA}, Val^{TAC}	21/22
3'tritsRNAs	3'tritRFs	Glu^{TTC}, Val^{TAC}, Lys^{CTT}	24
	3'tritRFs	Arg^{CCT}, Arg^{TCT}, Glu^{CTC}	33
	3'tritRNA-halves	Leu^{CAA}, Val^{GAC}, Thr^{TGT}, Ile^{GAT}, Met^{CAT}	40

Figures

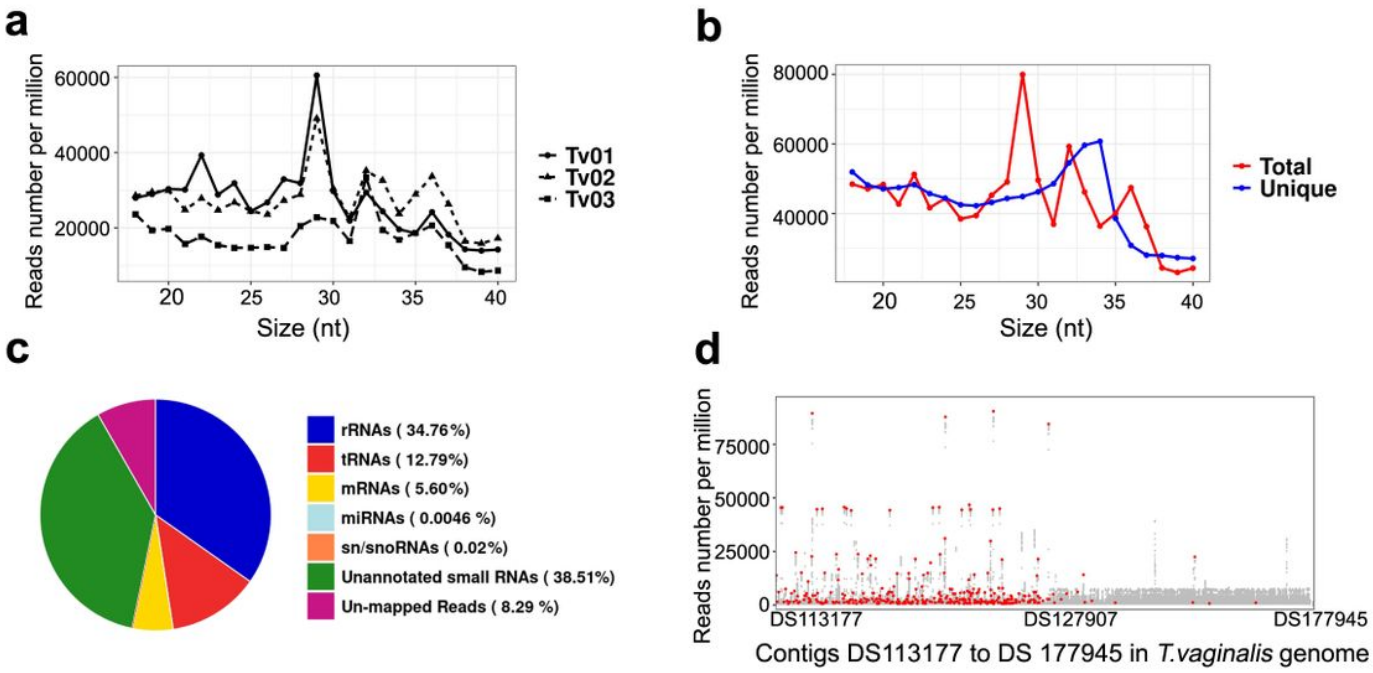

Figure 1

General features of 18-40 nt long small RNAs from T. vaginalis. a-b Size distributions of sRNAs from individual samples (a) and pooled data (b). c Abundance of small RNAs populations referring to the T. vaginalis genomic annotation. d Genome-wide density analysis of small RNAs along all contigs of T. vaginalis genome. Red dots represent tsRNAs.

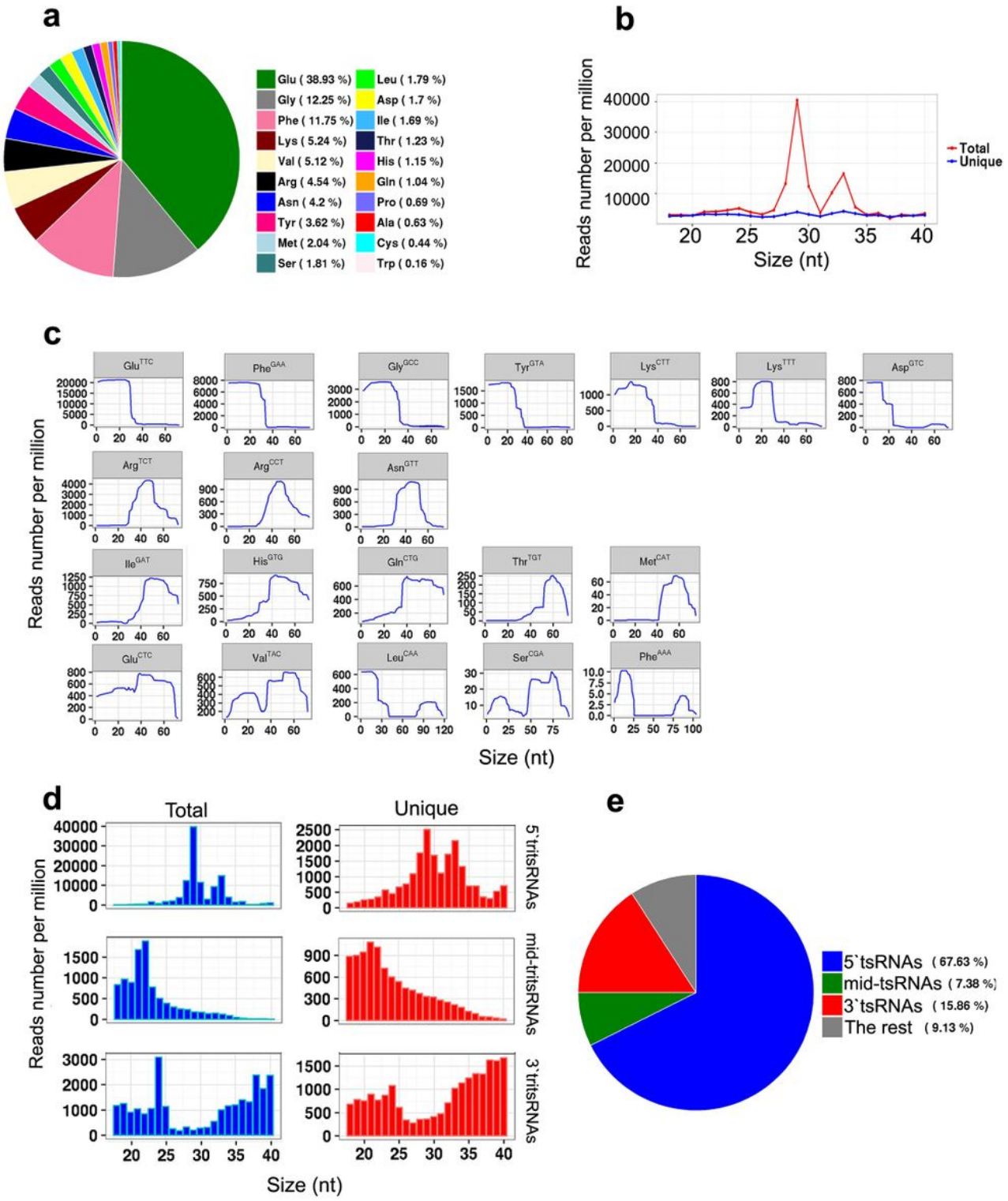

Figure 2

Profiles of tRNA-derived small RNAs from T. vaginalis. a Frequency of tsRNAs originated from tRNAs. b Size distributions of tsRNAs. c Coverage range analysis of tritsRNAs from top 20 highest tsRNAs-expressed tRNAs. d Size distributions of three types of tritsRNAs in both total and unique reads. e Frequency of three categories of tsRNAs.

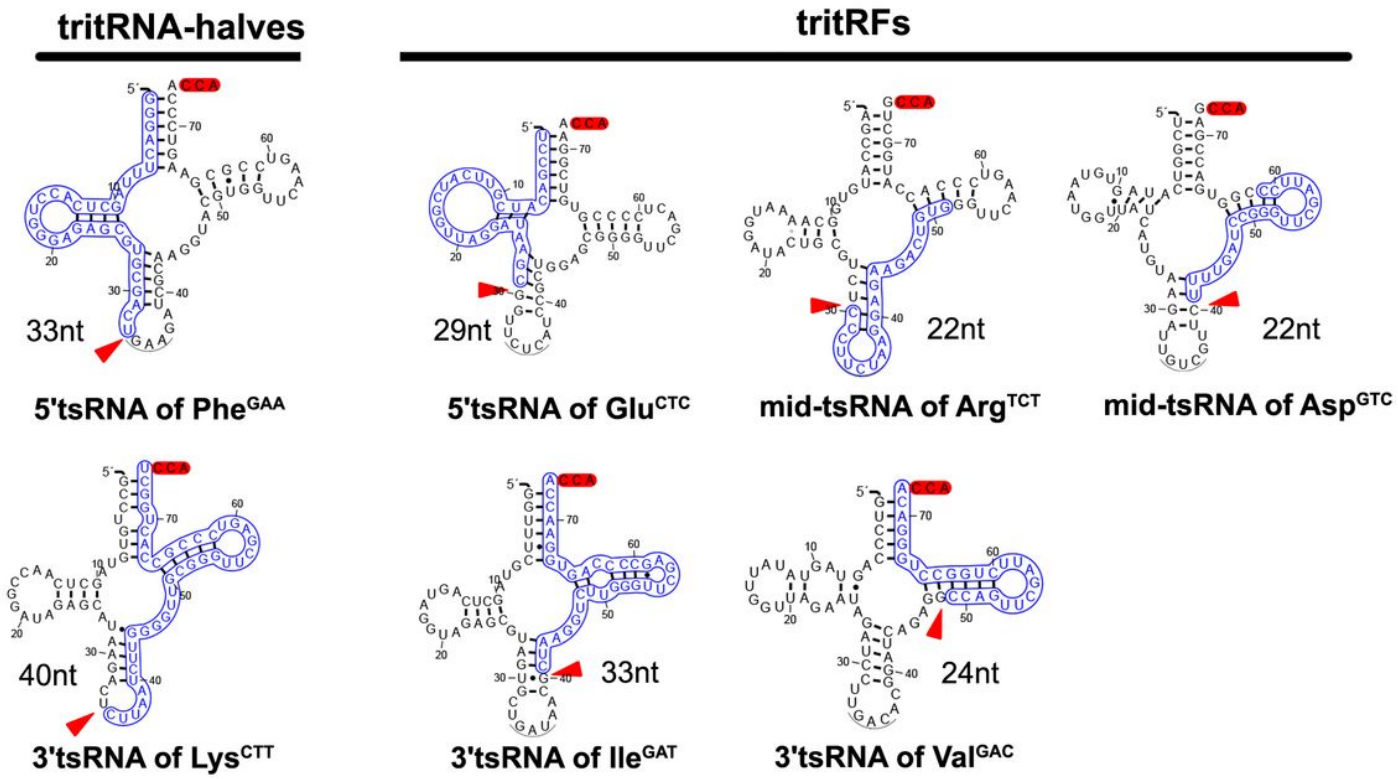

Figure 3

Cleavage sites of tritRNA-halves and tritRFs in schematic mature tRNAs. The tritsRNA sequences are highlighted in blue, and cleavage sites are indicated by red triangles.

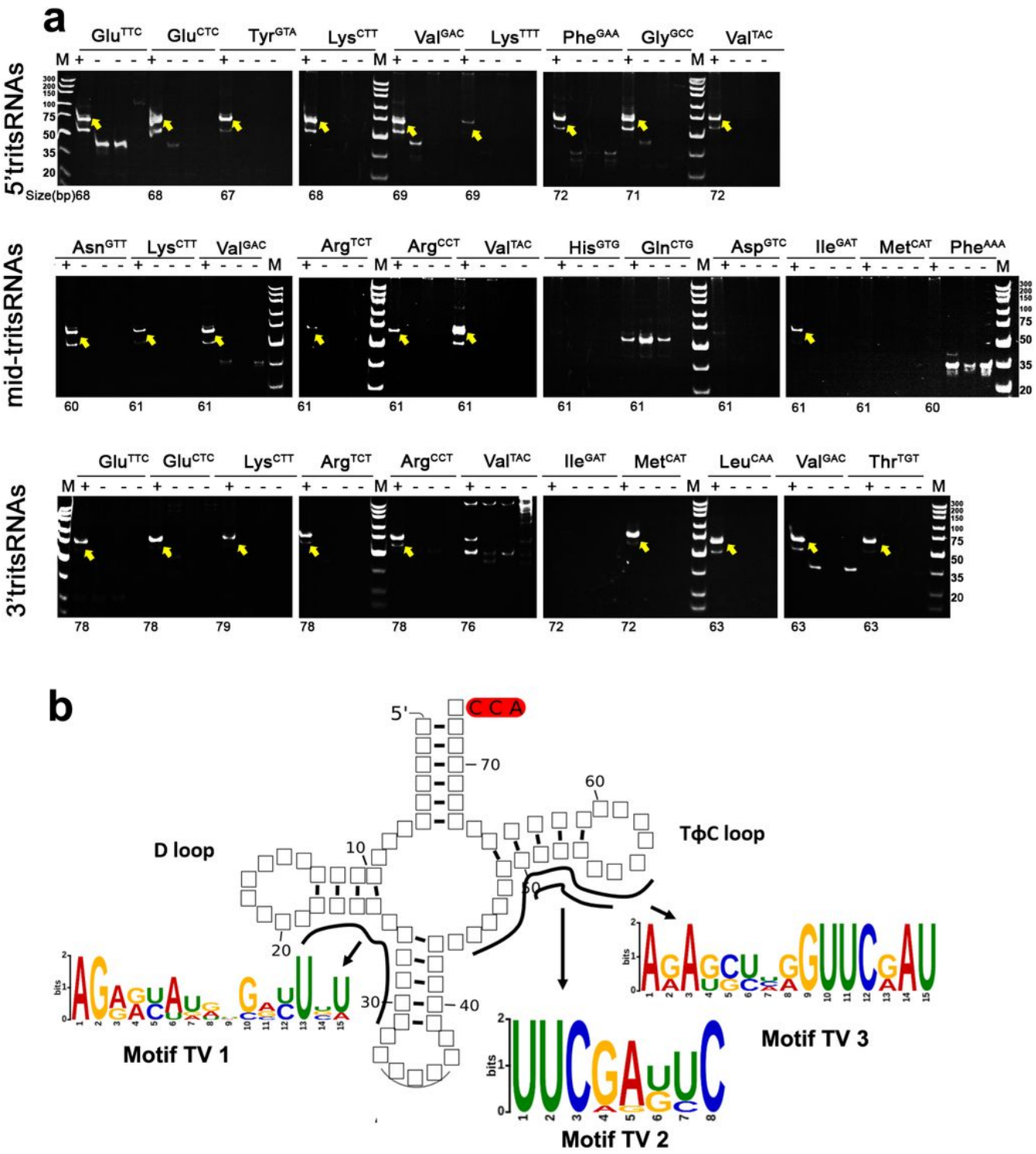

Figure 4

Experimental confirmation and motif prediction of tritsRNAs. a RT-PCR validation of tritsRNA candidates. Each tritsRNA is shown in four adjacent lanes. From left to right represents stem-loop RT-PCR with DNase-treated RNA template (left, “+”), without RNA template (left middle, “-”), without reverse transcriptase in RT reactions (right middle, “-”), and without template in PCR reaction as negative control (right, “-”). “M”

indicates DNA ladder. The yellow arrows illustrate the products with expected size. b Schematic representation of the motif sequences and locations in the backbone of a mature tRNA.

Supplementary Files

This is a list of supplementary files associated with this preprint. Click to download.

- FigureS1.jpg
- FigureS2.jpg
- FigureS3.jpg
- FigureS4.jpg
- additionalfile1.docx